

# Antifragility Predicts the Robustness and Evolvability of Biological Networks through Multi-class Classification with a Convolutional Neural Network

Hyobin Kim <sup>1</sup>, Stalin Muñoz <sup>1,2</sup>, Pamela Osuna <sup>1,3</sup>, and Carlos Gershenson <sup>1,4,5,\*</sup>

<sup>1</sup> Centro de Ciencias de la Complejidad, Universidad Nacional Autónoma de México, 04510 CDMX

<sup>2</sup> Facultad de Ingeniería, Universidad Nacional Autónoma de México, 04510 CDMX, México

<sup>3</sup> Faculté des Sciences et Ingénierie, Sorbonne Université, 4 place Jussieu 75005 Paris, France

<sup>4</sup> Instituto de Investigaciones en Matemáticas Aplicadas y en Sistemas, Universidad Nacional Autónoma de México, 04510 CDMX, México

<sup>5</sup> ITMO University, St. Petersburg, 199034, Russian Federation

\* Correspondence: cgg@unam.mx

**Abstract:** Robustness and evolvability are essential properties to the evolution of biological networks. To determine if a biological network is robust and/or evolvable, the comparison of its functions before and after mutations is required. However, it has an increasing computational cost as network size grows. Here we aim to develop a predictor to estimate the robustness and evolvability of biological networks without an explicit comparison of functions. We measure antifragility in Boolean network models of biological systems and use this as the predictor. Antifragility is a property to improve the capability of a system through external perturbations. By means of the differences of antifragility between the original and mutated biological networks, we train a convolutional neural network (CNN) and test it to classify the properties of robustness and evolvability. We found that our CNN model successfully classified the properties. Thus, we conclude that our antifragility measure can be used as a significant predictor of the robustness and evolvability of biological networks.

**Keywords:** robustness; evolvability; antifragility; complexity; prediction; Boolean networks; gene regulatory networks; convolutional neural networks

---

## 1. Introduction

Robustness and evolvability are well known as essential properties to the evolution of biological systems [1-6]. As studying the relationship between the two properties is necessary for understanding how biological systems can withstand mutations and simultaneously generate genetic variations, numerous studies on their relationship have been done [7-11]. Robustness allows the existing functions to be preserved in the presence of mutations or perturbations, while evolvability enables new functions to be expressed to adapt to new environments [12-14]. To determine if a biological system is robust and/or evolvable, the comparison of its functions before and after internal perturbations is needed. Pragmatically, in Boolean networks used as gene regulatory network models, the definition of robust and evolvable networks has been established via the comparison of dynamic attractors (*i.e.*, stable steady states) before and after internal perturbations [14] based on numerical and experimental evidence showing that the attractors represent cell types or cell functions [15-17].

The definition of robustness and evolvability has been applied to a number of studies adopting Boolean network models in artificial life and systems biology [18-20]. However, the calculations for finding the attractors of the networks are computationally expensive since as the network size  $N$  grows, there is a combinatorial explosion of the state space (*i.e.*, the set of all possible states, whose size is  $2^N$ ). As an alternative to this approach, in some studies where large networks are explored,

they only focus on the attractors with the largest basins among all basins of attraction (*i.e.*, the sets of states leading to attractors) without obtaining all attractors [14, 19, 21]. However, in the case of extremely long transient state transitions, long attractor lengths, or evenly distributed basins of attraction, this does not work. Here we aim to develop a predictor of robustness and evolvability without the explicit comparison of the functions (*i.e.*, attractors), and thus applicable to large networks.

We use antifragility to estimate the robustness and evolvability of biological networks. Antifragility can be defined as the ability of a system to improve its functionality in the presence of external perturbations [22]. In the context of Boolean networks, it can be measured by our previous approach [23, 24], where antifragility is easily calculated by means of complexity computed from partial state transitions. With the differences of antifragility before and after internal perturbations, we train a CNN model and then test it to classify the properties of robustness and evolvability. We found that our model successfully classified both properties. Thus, we conclude that antifragility can be used as a significant predictor of robustness and evolvability.

Our predictor — antifragility — has many potential applications. It would be useful to systems and computational biologists studying the properties of large biological networks from a dynamical perspective. They could efficiently find out if the large networks are either robust or evolvable, or both with just our simply calculable measure without investigating how the functions (attractors) of the networks are changed before and after mutations. Also, understanding antifragility would be helpful for uncovering the mechanism of how biological systems acquired robustness and evolvability. Besides, our antifragility measure could be used as a control parameter to build robust and/or evolvable engineered systems.

## 2. Materials and Methods

### 2.1. Boolean Networks and Biological Systems

Boolean networks proposed by Kauffman as gene regulatory network models [25-27] have been extensively used in many areas including artificial life, robotics, and systems biology [28-34]. They are represented by nodes and links, where the nodes refer to genes, and the links point out interactions between genes. Each node has a binary state 0 (OFF) or 1 (ON). 0 means being inhibited, and 1 indicates being activated or gene expression. The state of a node is determined by update rules with the states of input nodes. Once the topology and the update schemes of node states are set, they are fixed.

If the links are randomly arranged, and the node states are updated by Boolean functions randomly assigned to each node, the networks are called Random Boolean networks (RBNs). RBNs are also known as Kauffman's *NK* Boolean networks, where *N* is the number of nodes and *K* is the number of links per node (self-links can be included). Meanwhile, the links and the update rules of Boolean network models of biological systems are determined by experiments and literature demonstrating actual relationships between genes (or proteins).

The Boolean network composed of *N* nodes has a state space, which is defined as the set of  $2^N$  state configurations with transitions among them. Regarding the state space, there are two important terms: one is *attractors*, and the other is *basins of attraction*. Attractors are state configurations repeated over time in a point or a limit cycle, and basins of attraction are the rest of the configurations going toward attractors. In Figure 1, an example RBN and its state space are presented.

In this study, we use different Boolean network models of 38 biological systems. All the biological networks have less than 30 nodes. Among them, the maximum number of nodes is 26. The maximal value allows full search of attractors and basins of attraction in the state space ( $2^{26}=67,108,864$  states). For networks having over 26 nodes, it is difficult to perform the full search due to computational limits. Table 1 shows information about the biological networks collected from a public platform for modeling biological networks, *Cell Collective*. In the table, the networks are sorted by their size.

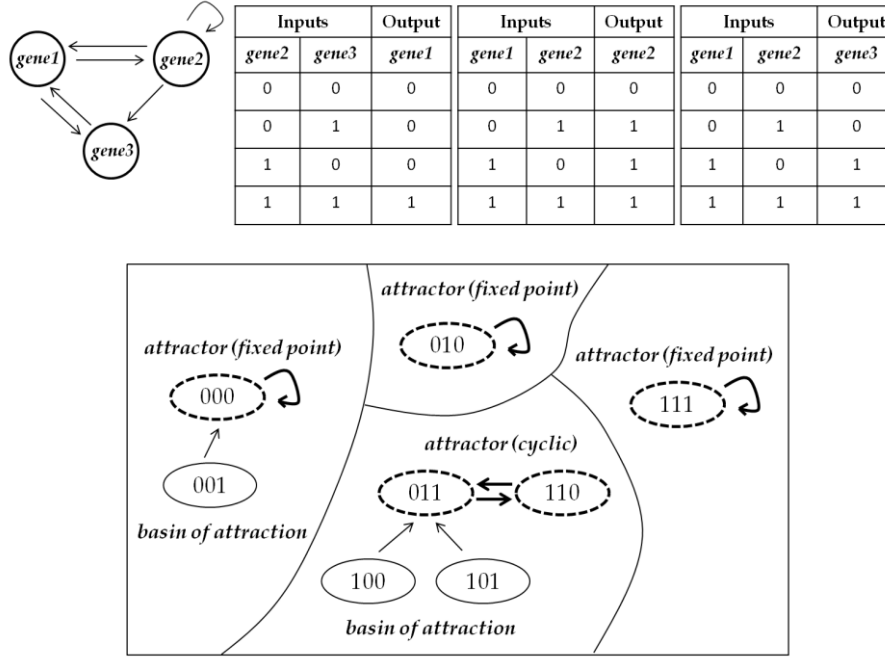


**Figure 1.** An example RBN with  $N=3$  and  $K=2$  and its state space. The topology is randomly determined and Boolean functions are randomly assigned to each node. The state space is composed of  $2^3=8$  state configurations from 000 to 111. In the state space, attractors are the configurations with bold dashed lines, and basins of attraction are the configurations except for the attractors.

**Table 1.** Different Boolean network models of 38 biological systems used for simulations.

Biological network <sup>1</sup>	Network size	Ref.
#1. Cortical area development (cortical)	5	[35]
#2. Cell cycle transcription by coupled CDK and network oscillators (cycle-cdk)	9	[36]
#3. Mammalian cell cycle (core-cell-cycle)	10	[37]
#4. Toll pathway of drosophila signaling pathway (toll-drosophila)	11	[38]
#5. Metabolic interactions in the gut microbiome (metabolic)	12	[39]
#6. Regulation of the L-arabinose operon of Escherichia coli (l-arabinose-operon)	13	[40]
#7. Lac operon (lac-operon-bistability)	13	[41]
#8. Arabidopsis thaliana cell-cycle (arabidopsis)	14	[42]
#9. Predicting variabilities in cardiac gene (gene-cardiac)	15	[43]
#10. Cardiac development (cardiac)	15	[44]
#11. Fanconi anemia and checkpoint recovery (anemia)	15	[45]
#12. HCC1954 breast cell line short-term ErbB network (hcc1954-ErbB)	16	[46]
#13. BT474 breast cell line short-term ErbB network (bt474-ErbB)	16	[46]
#14. Neurotransmitter signaling pathway (neurotransmitter)	16	[47]
#15. SKBR3 breast cell line short-term ErbB network (skbr3-short)	16	[46]
#16. Body segmentation in drosophila (body-drosophila)	17	[48]
#17. Budding yeast cell cycle (budding-yeast)	18	[49]
#18. VEGF pathway of drosophila signaling pathway (vegf-drosophila)	18	[38]
#19. CD4 <sup>+</sup> T cell differentiation and plasticity (cd4)	18	[50]
#20. T-LGL survival network (t-lgl-survival)	18	[51]
#21. Human gonadal sex determination (gonadal)	19	[52]
#22. Oxidative stress pathway (oxidative-stress)	19	[53]
#23. Budding yeast cell cycle (yeast-cycle)	20	[54]
#24. Mammalian cell-cycle (mammalian)	20	[55]

#25. <i>B cell differentiation (b-cell)</i>	22	[56]
#26. <i>Iron acquisition and oxidative stress response in aspergillus fumigatus (aspergillus-fumigatus)</i>	22	[57]
#27. <i>Aurora kinase A in neuroblastoma (aurka)</i>	23	[58]
#28. <i>FGF pathway of drosophila signaling pathways (fgf-drosophila)</i>	23	[38]
#29. <i>T cell differentiation (t-cell-differentiation)</i>	23	[59]
#30. <i>Processing of Spz Network from the drosophila signaling pathway (spz-drosophila)</i>	24	[38]
#31. <i>TOL regulatory network (tol)</i>	24	[60]
#32. <i>HH pathway of drosophila signaling pathways (hh-drosophila)</i>	24	[38]
#33. <i>BT474 breast cell line long-term ErbB network (bt474)</i>	25	[46]
#34. <i>SKBR3 breast cell line long-term ErbB network (skbr-long)</i>	25	[46]
#35. <i>HCC1954 breast cell line long-term ErbB network (hcc1954)</i>	25	[46]
#36. <i>Wg pathway of drosophila signaling pathways (wg-drosophila)</i>	26	[38]
#37. <i>Trichostrongylus retortaeformis (trichostrongylus)</i>	26	[61]
#38. <i>Pro-inflammatory tumor microenvironment in acute lymphoblastic leukemia (leukemia)</i>	26	[62]

<sup>1</sup> Data was collected from *Cell Collective* (<https://research.cellcollective.org/?dashboard=true#>).

## 2.2. Mutations and Classification of Robustness & Evolvability

We introduce mutations to the biological networks and study their robustness and evolvability. As the internal perturbations, we randomly add, delete one regulatory link, change the position of a link in the network, or flip a state in a Boolean function [63-65]. Comparing the attractors between the original and mutated networks, we classify the properties of biological networks into four classes [66]: *not robust & not evolvable*, *not robust & evolvable*, *robust & not evolvable*, and *robust & evolvable*. This is classification extended from the definition of robust and evolvable network in Aldana's work [14] as described below.

Figure 2 schematically illustrates the four classes of robustness and evolvability. If the mutated network does not have full attractors of the original one and further does not produce any new attractors, it is classified as *not robust & not evolvable*. If the mutated network does not fully have original attractors but creates new attractors, it is classified as *not robust & evolvable*. If the mutated network maintains the original attractors but does not generate any new attractors, it is classified as *robust & not evolvable*. If the mutated network has the same attractors as the original one and simultaneously produces new attractors, it is classified as *robust & evolvable*.

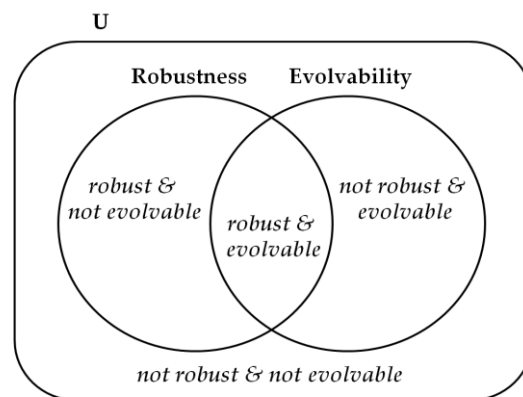


**Figure 2.** The schematic diagram of the four classes on robustness and evolvability. Depending on the change of attractors between original and mutated networks, the network is certainly classified into one class among *not robust & not evolvable*, *not robust & evolvable*, *robust & not evolvable*, and *robust & evolvable*.

In our simulations, we independently add an internal perturbation 20,000 times to each network, and then get 20,000 perturbed networks per biological network. Next, we classify the properties of all the perturbed networks into the above four classes. Since one biological network can be *not robust & not evolvable*, *not robust & evolvable*, *robust & not evolvable*, or *robust & evolvable* against the 20,000 perturbations, we can get the percentage frequency distribution of the four classes per network.

### 2.3. Antifragility in Boolean Networks

The definition of antifragility was established by Taleb [22]. Antifragility is a property not only to withstand external perturbations but also to improve the capabilities of systems exposed to them. In Boolean networks, the property can be computed in our previous studies [23, 24]. On the assumption that antifragility implying responses to external perturbations might be helpful to predict responses to internal perturbations, we use here antifragility as a predictor to estimate the robustness and evolvability of biological networks against mutations. To understand our antifragility measure, first grasping complexity and external perturbations is required.

#### 2.3.1. Complexity of Boolean networks

Complexity is defined as a balance between change and regularity [26]. On the basis of the concept, we defined emergence and self-organization representing change and regularity, and presented a measure to quantify complexity using them in our earlier studies [67, 68]. Complexity ( $C$ ) is calculated from emergence ( $E$ ) and self-organization ( $S$ ) as follows:

$$C = 4 \times E \times S, \quad (1)$$

where coefficient 4 is added to normalize the values of  $C$  to the range of  $[0,1]$  ( $0 \leq C \leq 1$ ). Because  $S$  can be regarded as the complement of  $E$  [67, 68], equation (1) is reformulated by the following equation:

$$C = 4 \times E \times (1 - E), \quad (2)$$

In a Boolean network which consists of  $N$  nodes,  $E$  ( $0 \leq E \leq 1$ ) is measured as the average of emergence values for all nodes, where the emergence of each node is computed through Shannon's information entropy:

$$E = \frac{\sum_{i=1}^N E_i}{N} = \frac{\sum_{i=1}^N -(p_0^{(i)} \log_2 p_0^{(i)} + p_1^{(i)} \log_2 p_1^{(i)})}{N}, \quad (3)$$

where  $p_0^{(i)}$  ( $p_1^{(i)}$ ) is the ratio of how many 0s (1s) are expressed to  $T$  state transitions for node  $i$  (*i.e.*,  $p_0^{(i)} + p_1^{(i)} = 1$ ). Regarding  $T$ , focusing on state transitions not from 1 to  $T$  but from  $T+1$  to  $2T$ , we obtain  $p_0^{(i)}$  ( $p_1^{(i)}$ ). This is because we can calculate more stable value of  $p_0^{(i)}$  ( $p_1^{(i)}$ ) by getting state transitions closer to attractors. Figure 3 displays an example of computing  $E$  in a Boolean network.

In equation (2),  $C$  has the maximum value of 1 when  $E$  is 0.5 [68, 69]. For example, under the condition that all the nodes of a Boolean network have the same emergence values, when  $p_0$  or  $p_1$  is around 0.89, average  $E$  becomes 0.5. In contrast,  $C$  has the minimum value of 0 when  $E$  is 1 or 0. In the same condition above, when  $p_0$  and  $p_1$  are 0.5 or when  $p_0$  or  $p_1$  is 1, average  $E$  becomes 1 or 0. As seen in the examples, complexity is determined by how 0s and 1s are distributed during state transitions. In other words, complexity indicating a balance between change and regularity is assessed by the distribution of node states resulting from the processes of altering and keeping the node states in Boolean networks.

#### 2.3.2. External perturbations to Boolean networks

We consider flipping the node states of the networks external perturbations so as to measure antifragility [23, 24]. The degree of external perturbations ( $\Delta x$ ) is quantified by the following equation:

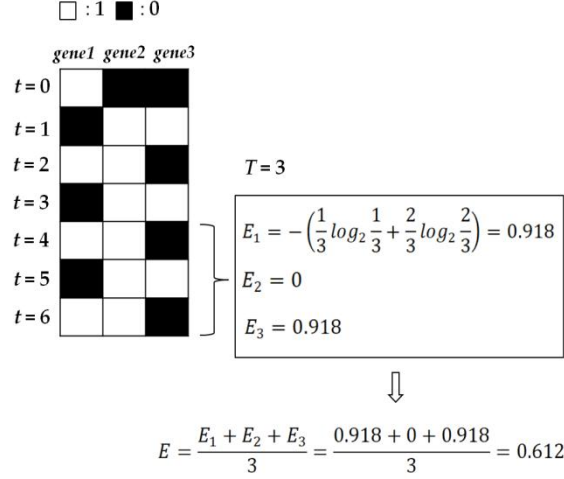


**Figure 3.** An example showing how to calculate the emergence of each node and the average,  $E$ . With initial configuration 100, the state transitions were obtained from  $t=0$  to  $t=6$  in the example RBN of Figure 1.

$$\Delta x = \frac{X \times (\frac{T}{O})}{N \times T}, \quad (4)$$

where  $X$  is the number of nodes randomly chosen for the perturbations,  $T$  is the simulation time for state transitions, and  $O$  is the perturbation frequency. For instance, if  $N=10$ ,  $X=4$ ,  $T=5$ , and  $O=1$ , we randomly choose 4 nodes in a network with 10 nodes and then change the states of the nodes. We repeat this perturbation every time step during  $2 \times 5 = 10$  time steps (Here, perturbing the network during not 5 but 10 timesteps is because we are interested in state transitions from  $T+1$  to  $2T$  as mentioned in 2.3.1).

$\Delta x$  has the interval  $[0,1]$  ( $0 \leq \Delta x \leq 1$ ). This term is used in order to adjust the influence of network size on antifragility. In the simulations, the parameters are set to  $X=[1, 2, \dots, N]$ ,  $T=200$ , and  $O=1$ . The values of  $T$  and  $O$  are determined based on our previous research [23]:  $T=200$  was enough to measure antifragility of Boolean networks which have less than 100 nodes, and  $O=1$  showed the most distinctive difference of antifragility between networks.

### 2.3.3. Antifragility of Boolean networks

Our antifragility measure ( $\phi$ ) is composed of two terms: the difference of “satisfaction” before and after external perturbations ( $\Delta\sigma$ ) and the degree of external perturbations ( $\Delta x$ ) [23, 24]. The equation is as follows:

$$\phi = -\Delta\sigma \times \Delta x, \quad (5)$$

Here we describe only  $\Delta\sigma$  because  $\Delta x$  was explained in 2.3.2. To obtain  $\Delta\sigma$ , it is needed to understand the concept of satisfaction ( $\sigma$ ).  $\sigma$  represents how much the “goal” of agents has been attained [70]. The agents and goal can be differently defined depending on systems. In Boolean networks, each node can be regarded as an agent. It can be said that their goal is to achieve high complexity.

In equation (5),  $\Delta\sigma$  is calculated by the following equation:

$$\Delta\sigma = C - C_0, \quad (6)$$

where  $C_0$  and  $C$  point out complexity before and after external perturbations respectively.  $\Delta\sigma$  has values in the range  $[-1,1]$  ( $-1 \leq \Delta\sigma \leq 1$ ) as  $C_0$  and  $C$  have the interval  $[0,1]$ . Thus, if  $\Delta\sigma$  is positive ( $C \geq C_0$ ), it means that complexity increases by external perturbations. That is, we define “benefiting from perturbations” as increasing their complexity. If this is the case, the Boolean network can be considered *antifragile*. If  $\Delta\sigma$  is negative ( $C \leq C_0$ ), it indicates that complexity

decreases by external perturbations. It can be seen as *fragile*. If  $\Delta\sigma$  is zero ( $C = C_0$ ), complexity is maintained against external perturbations. It can be regarded as *robust*.

To calculate  $C_0$  and  $C$ , when the state transitions of the original network and perturbed one are computed, the same initial states are used at  $t=0$ . Depending on the initial states, because complexity can be different,  $C_0$  and  $C$  are calculated as the average of the complexity values acquired from a large number of initial conditions that are randomly chosen. This allows more stable value of  $\phi$  as a system property. In the simulations, the number of initial states ( $s$ ) is set to 1,000.

## 2.4. Property Classification with a Convolutional Neural Network

### 2.4.1. Input and output in a CNN

We use a CNN to classify the properties of the biological networks into the four classes: *not robust & not evolvable*, *not robust & evolvable*, *robust & not evolvable*, and *robust & evolvable*. In our CNN model, its input is the differences of antifragility between original and mutated networks, and its output is the properties classified into the four classes. As we use 38 biological networks and add the internal perturbations 20,000 times to each network, we have  $38 \times 20,000 = 760,000$  quantities of the differences of antifragility and the classified properties, respectively.

When we get the input, let's take the *Mammalian cell cycle* network with 20 nodes and its mutated network as an example. Figure 4(a) and 4(b) show the antifragility of the two networks depending on the number of perturbed nodes  $X$ . We interpolate to get 30 data points for each network and subtract the antifragility value of the mutated network from that of the original network at each data point. Then, we get 30 difference values in the normalized range  $[1/N, 1 (=N/N)]$  (Figure 4(c)). In this way, for all the networks with the different number of nodes, we can get 760,000 input elements in which one element is composed of 30 data points. This process for the input is because CNNs require same size inputs.

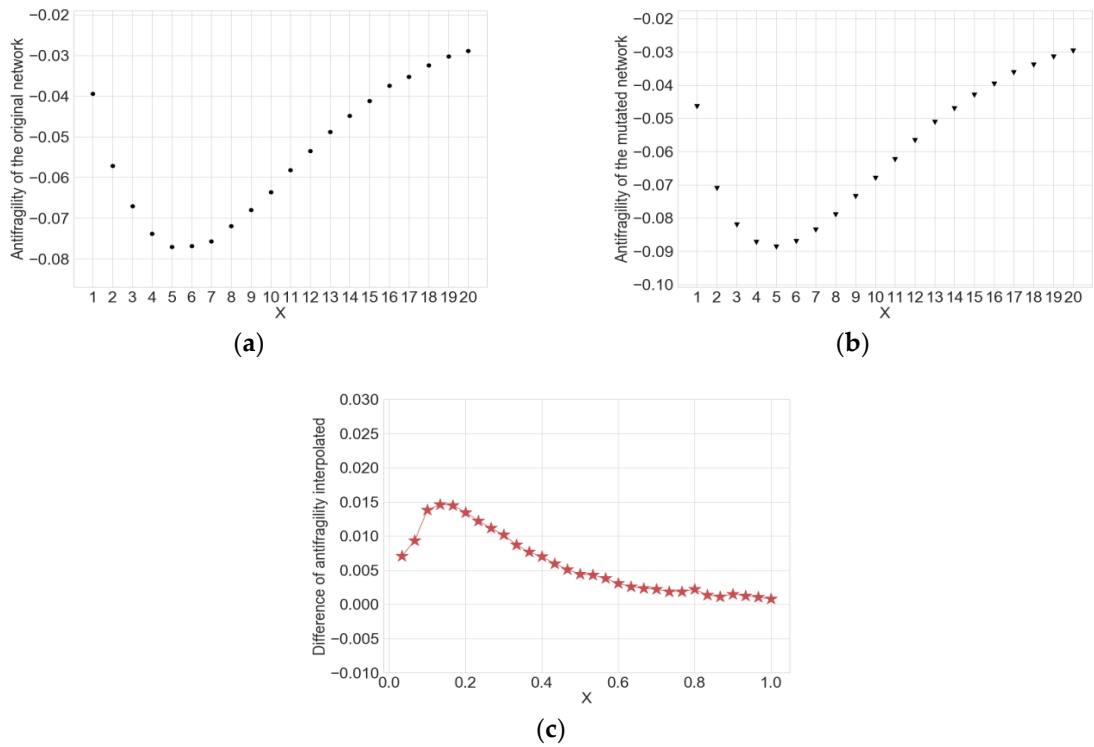


**Figure 4.** Data points related to antifragility of the *mammalian cell cycle* network with  $N=20$ . In the simulations, the parameters were set to perturbed node size  $X=[1, 2, \dots, 20]$ , simulation time for state transitions  $T=200$ , perturbation frequency  $O=1$ : (a) 20 data points on antifragility of the original network; (b) 20 data points on antifragility of the mutated network; (c) 30 data points on the differences of antifragility estimated through interpolation in the normalized range.

### 2.4.2. Training and testing data sets and parameter settings for simulations

We split the data with the 760,000 quantities into training data (*i.e.*,  $760,000 \times 0.7 = 532,000$ ) and test data (*i.e.*,  $760,000 \times 0.3 = 228,000$ ) with the ratio of 70 to 30. However, the data about the properties labeled with the four classes is imbalanced, as the four classes are not equally distributed. Thus, we have multiclass classification with imbalanced data. We make the training data balanced using Synthetic Minority Over-sampling Technique (SMOTE) which is an oversampling technique generating synthetic samples from the minority class [71]. We get balanced data that make up of the same number of samples per class. Then, we train the model with the balanced data and test it with the original imbalanced data.

Figure 5 shows our CNN architecture. Our CNN model has two consecutive convolution layers, one pooling layer, and two fully connected layers. We set to kernel size=3 and number of output filters=64 in the first convolution layer with no activation function and the second convolution layer with a ReLU function. Next, we use max pooling with window size=2 in the pooling layer. We flatten the output from the pooling layer and then send it to the fully connected layers. The first fully connected layer consists of 100 nodes, which is activated by a ReLU function. The second one is our output layer with a soft-max function. The number of nodes is the same size as the number of our classes. For simulations, we set to batch size=512 and maximum epochs=150 with early stopping to avoid overfitting. Finally, we get a test accuracy, a confusion matrix, and precision-recall (PR) curves to evaluate the model performance.

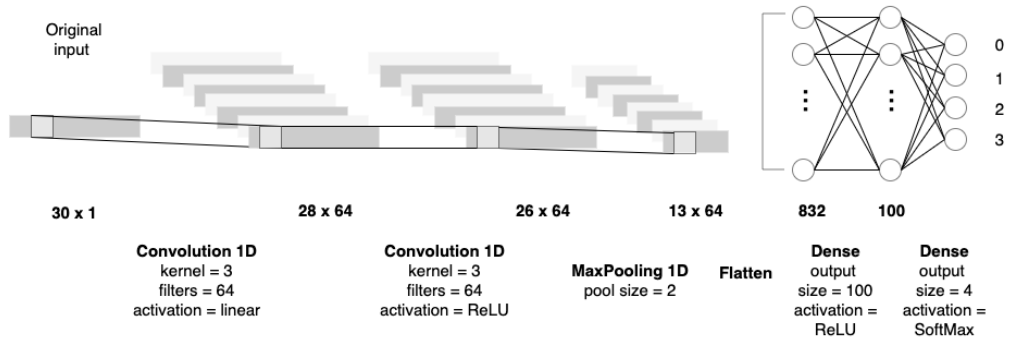


**Figure 5.** CNN architecture for simulations. Our CNN model is composed of two convolution layers, one pooling layer, and two fully connected layers.

## 3. Results

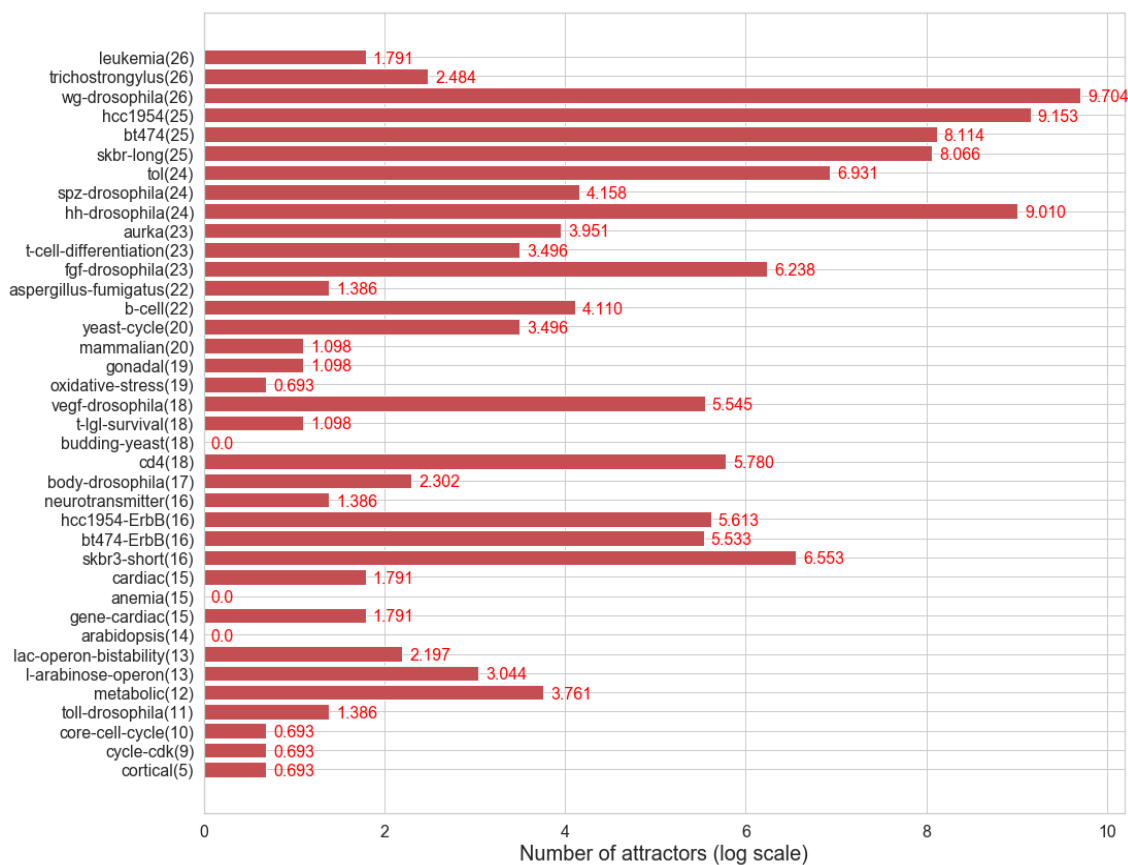
### 3.1. Attractors and Basins of Attraction of Biological Networks

We looked into the attractors and basins of attraction to find the structural features of the state space in the Boolean network models of the 38 biological systems. Specifically, we measured the number of attractors, the average length of attractors, and the normalized basin entropy. In the case of the normalized basin entropy, it was calculated as dividing Krawitz et al.'s basin entropy [72] by the number of nodes (*i.e.*,  $H = -\sum_{\rho} p_{\rho} \log_2 p_{\rho} / N$  where  $p_{\rho}$  is the basin size of attractor  $\rho$  divided by state space size  $2^N$ ,  $\sum_{\rho} p_{\rho} = 1$ ). It is normalized between 0 and 1. As mentioned in the introduction, the attractors can represent cell types or functions [15-17]. Hence, from a biological viewpoint, the number of attractors can be interpreted as the number of cell functions, the average length of attractors can be regarded as the time that it takes cell functions to be conducted, and the normalized basin entropy can be seen as the versatility of cell functions.

Figure 6(a) shows the distribution of the number of attractors with the values varied between 1 and 16,384. It means that the cell functions which are carried out are different per biological system. Figure 6(b) displays the distribution of the average length of attractors. Overall, more than half of the networks have a fixed-point attractor, and the rest of them have relatively short cyclic attractors when their state space sizes are considered. However, the values are still varied between

1 and 11. It implies that the cell functions of the biological systems have different operating times but never too long. Figure 6(c) presents the distribution of the normalized basin entropy. The larger it is, the more evenly distributed the basins are. The values are diversely distributed between 0 and 0.6. It indicates that some biological systems perform only a few cell functions dominantly, while others commonly change the cell functions among many ones.

All the three measures have large variations between the values, so it is hard to find the common structural features of the state space. This would have resulted from the characteristics of the cell functions of the biological systems and the scale of modeling. From the variations, we can see that there exist biological networks that have so many number of attractors, long attractor lengths, and/or evenly distributed basins. For these networks, it is practically difficult to study the robustness and evolvability of biological systems by comparing the attractors before and after perturbations. It is even harder for larger biological networks because the number of attractors, the attractor length, and the basin size will increase as the number of nodes grows. Therefore, it is necessary to efficiently estimate the robustness and evolvability of biological networks without checking the attractors.



(a)

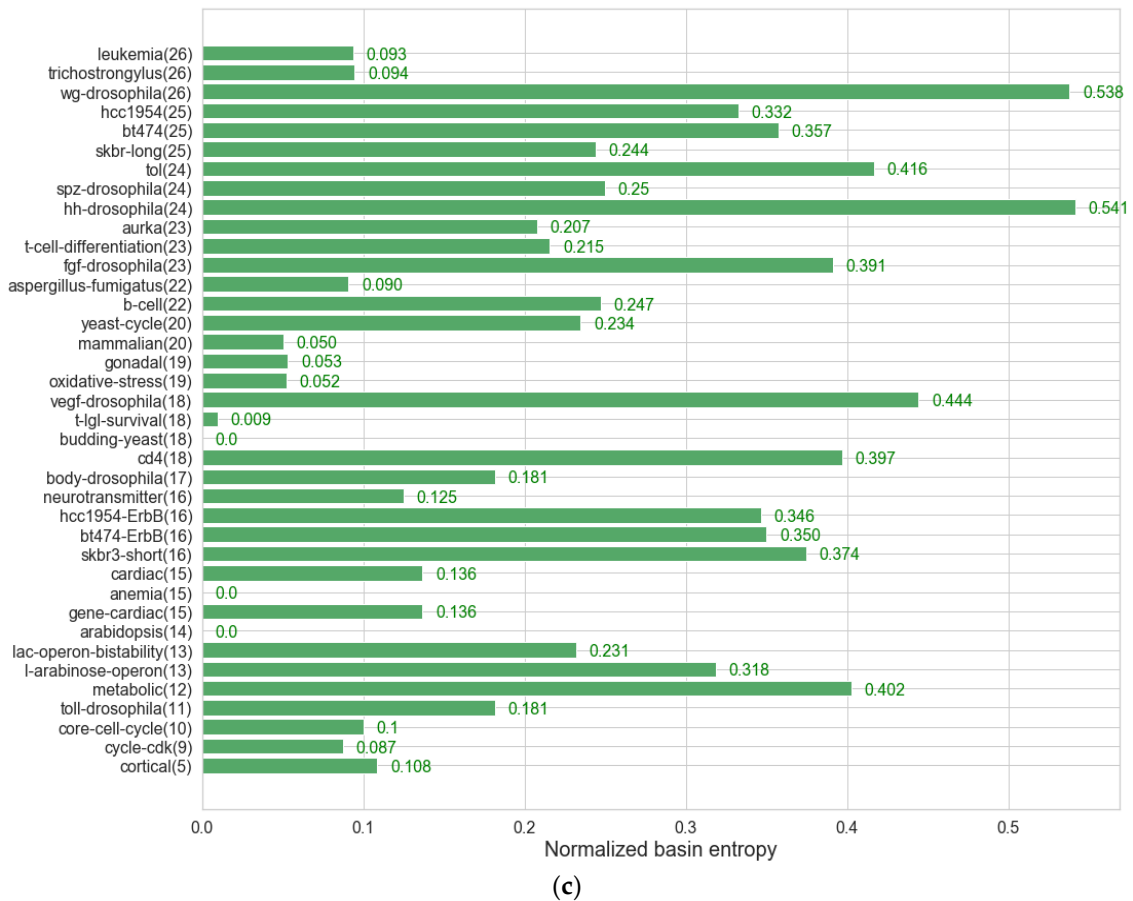
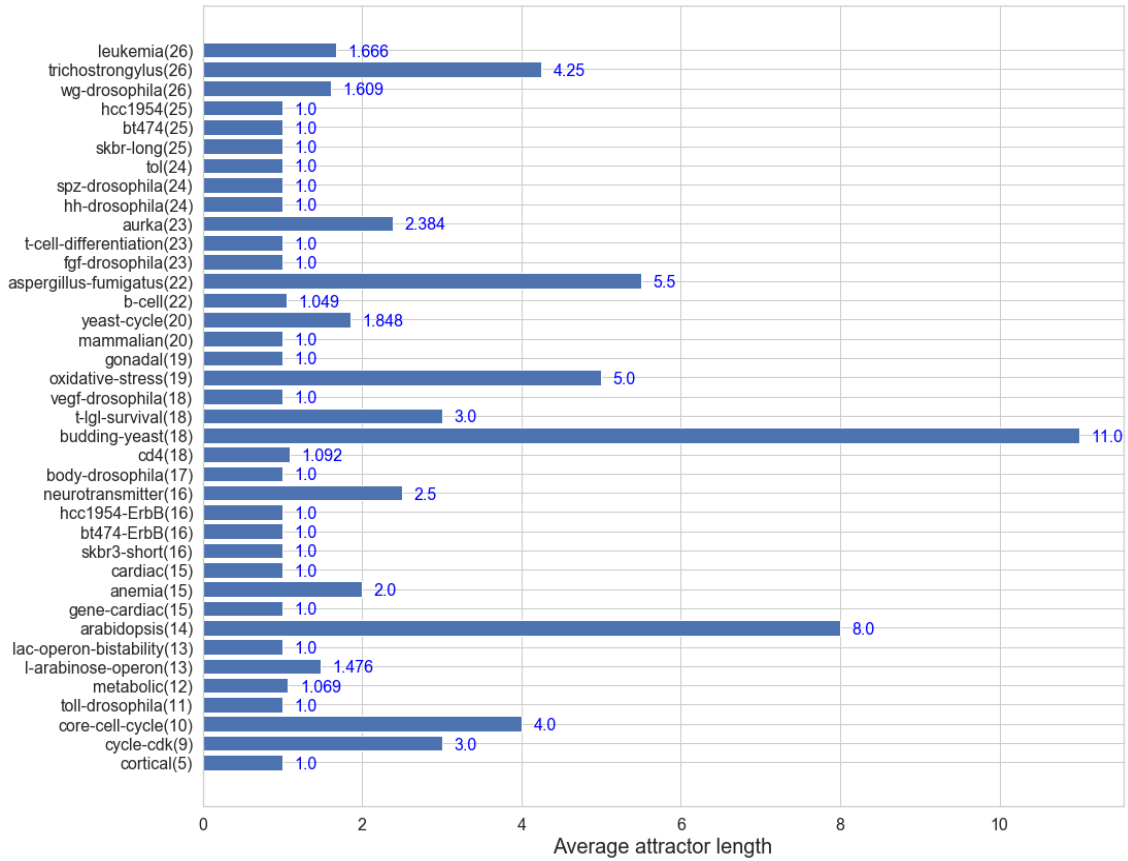


**Figure 6.** Attractors and basins of attraction of the 38 biological networks. The number in the parenthesis on the y-axis points out the number of nodes of the network: (a) The number of attractors. The values took the natural logarithm.; (b) The average length of attractors; (c) Normalized basin entropy. It has the range of [0,1]. The larger the value is, the more evenly distributed the basins are.

### 3.2. Distribution of the Four Classes on Robustness & Evolvability of Biological Networks

We classified the robustness and evolvability of the 38 biological networks into the four classes (*not robust & not evolvable*, *not robust & evolvable*, *robust & not evolvable*, *robust & evolvable*) to investigate how the biological networks respond to mutations. Figure 7 shows the percentage frequency distribution of the four classes. For each biological network, we added the internal perturbation 20,000 times, and thus acquired the percentage frequency from the 20,000 mutated networks.

As seen in the figure, every biological network has two, three, or four classes, which means that each biological system shows different behaviors against mutations. In fact, most of the biological networks are seldom classified into *robust & evolvable*, but rather classified into *not robust & evolvable* and *robust & not evolvable*. These findings propose one possible interpretation that the robustness and evolvability of biological systems [1-6] are not deterministic but stochastic responses to mutations. Furthermore, the robustness and evolvability of biological systems might be able to be explained from dynamically showing either the behavior that only original cell functions are maintained without new cell functions, or the behavior that new cell functions are created with original cell functions impaired. It can also be argued that a more complex mechanism is required for being at the same time *robust & evolvable*, so this could explain why not many networks exhibit both properties frequently.

In addition, such distribution of the dynamical responses suggests evolutionary profiles of what the environments given to the biological systems were like. *not robust & evolvable* makes up the highest percentage frequency of the four classes in the distribution, which implies that many biological systems might have been mainly exposed to drastic environmental changes hard to keep existing cell functions, and thus evolved towards preferring producing brand new cell functions to adapt to the new environments.

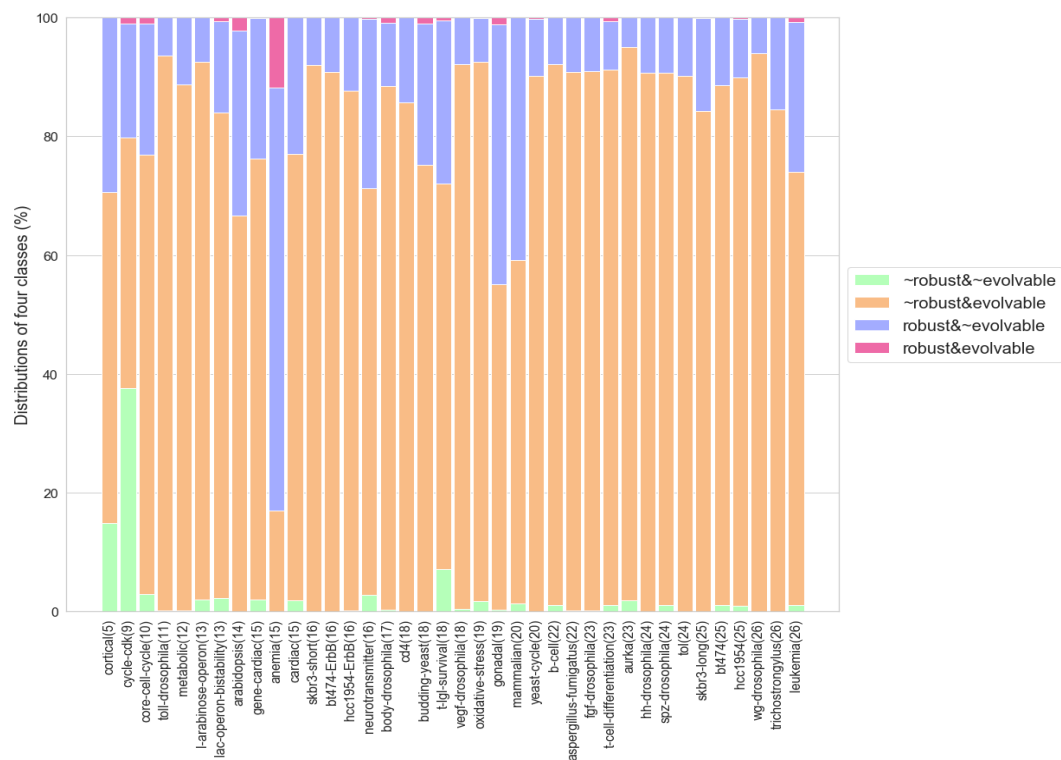


**Figure 7.** Percentage frequency distribution of the four classes on robustness and evolvability for the 38 biological networks. The internal perturbation was added to each network 20,000 times so 20,000 mutated networks were generated per biological network. The perturbed ones were classified into *not robust & not evolvable*, *not robust & evolvable*, *robust & not evolvable*, or *robust & evolvable*.

### 3.3. Association Between Mutation Type and Robustness & Evolvability

We computed Cramer's V to measure the strength of association between the mutation type and the robustness and evolvability. We had the four mutation types: adding a link (*add*), deleting a link (*delete*), changing the position of a link (*change*), and flipping one state in a Boolean function (*flip*). We randomly chose one mutation type and then added it to the biological network. This process was repeated 20,000 times per biological network, so we obtained 760,000 pairs (mutation type, property class) for the 38 biological networks. Table 2 is a contingency table displaying the frequency distribution of the four classes depending on the mutation type. From the table, we got Cramer's V=0.105. Cramer's V takes values from 0 to 1. The closer to zero the value is, the weaker association between the variables is. Hence, we found that there is almost no association between the mutation type and the property class. It indicates that genetic mutations do not have an effect on determining the robustness and evolvability of biological systems.

**Table 2.** A contingency table for the four classes depending on the mutation type.

	<i>add</i>	<i>delete</i>	<i>change</i>	<i>flip</i>
<i>not robust &amp; not evolvable</i>	2471	6446	4563	3946
<i>not robust &amp; evolvable</i>	144387	168008	156360	138332
<i>robust &amp; not evolvable</i>	42082	14460	27648	46794
<i>robust &amp; evolvable</i>	1271	871	1379	982

### 3.4. Prediction of Robustness & Evolvability Using Antifragility

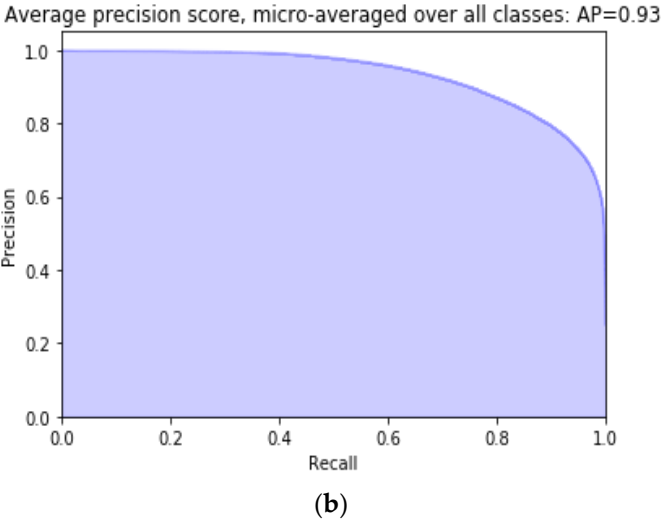
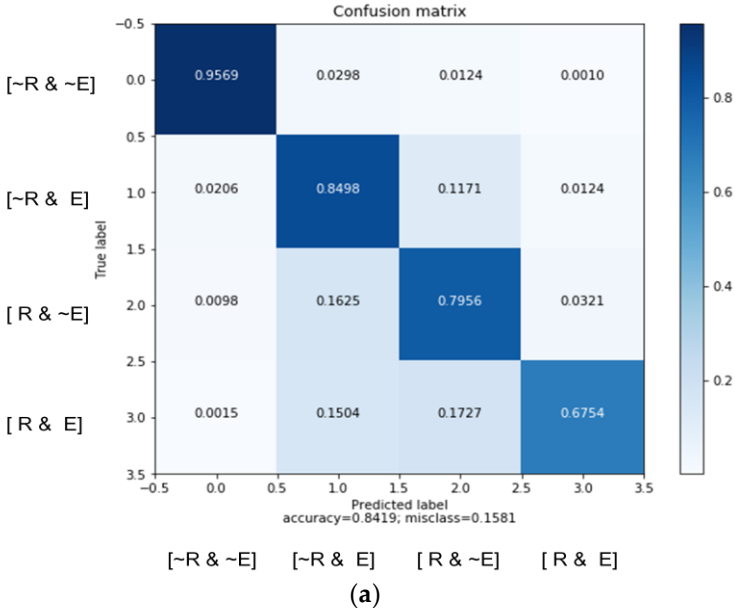
We got a test accuracy, confusion matrix, and precision-recall curves to evaluate the performance of our CNN model. We preferred using precision-recall (PR) curves to receiver operating characteristic (ROC) curves because we tested the model with the imbalanced data.

Figure 8(a) presents a test accuracy and normalized confusion matrix. The overall accuracy is 0.8419. In the confusion matrix, the x-axis refers to an instance of the predicted classes, and the y-axis represents an instance of the actual classes. The values of the diagonal elements mean the probability of correctly predicted classes. For each class, *not robust & not evolvable* is 0.9569, *not robust & evolvable* is 0.8498, *robust & not evolvable* is 0.7956 and *robust & evolvable* is 0.6754. From the accuracy and confusion matrix, we can see that our model has a great performance for the classification of robustness and evolvability.

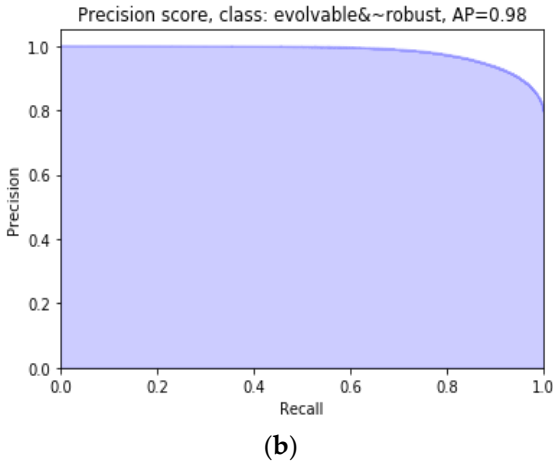
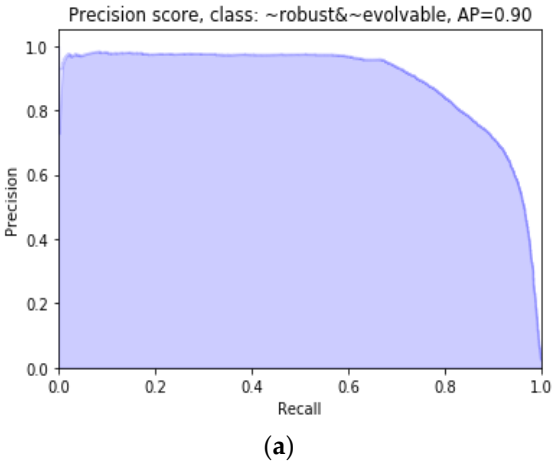
Figure 8(b) exhibits a micro averaged PR curve for the four classes. We computed the micro average globally not distinguishing the elements between different classes, which is usually preferable for imbalanced classes. In our PR curve, the area under the curve is AP=0.93. The large AP means high precision and high recall. High precision is related to a low false positive rate (type I error  $\alpha$ ) and high recall is related to a low false negative rate (type II error  $\beta$ ). Thus, the high AP values demonstrates that our model is a good classifier.

Overall, our model has a good performance but there are differences for each class. Figure 9 shows PR curves per class. *not robust & not evolvable* has AP=0.90 (Figure 9(a)), *not robust & evolvable* has AP=0.98 (Figure 9(b)), *robust & not evolvable* has AP=0.72 (Figure 9(c)), and *robust & evolvable* has AP=0.44 (Figure 9(d)). *not robust & not evolvable* and *not robust & evolvable* have large AP values, and also the AP value of *robust & not evolvable* is quite large. It represents that not only a majority of the properties for the three classes are detected but also they are correctly classified. However, *robust & evolvable* has the smaller AP value when compared to the other classes. It might be resulted from the scarcity of data on *robust & evolvable* as seen in Figure 7, and/or a high variance of the differences of

antifragility classified into *robust & evolvable*. The two things might have made it hard for our CNN model to find the feature map of *robust & evolvable*.



**Figure 8.** Model evaluation: (a) Normalized confusion matrix; (b) micro-averaged precision-recall curve for the four classes and its average precision score.



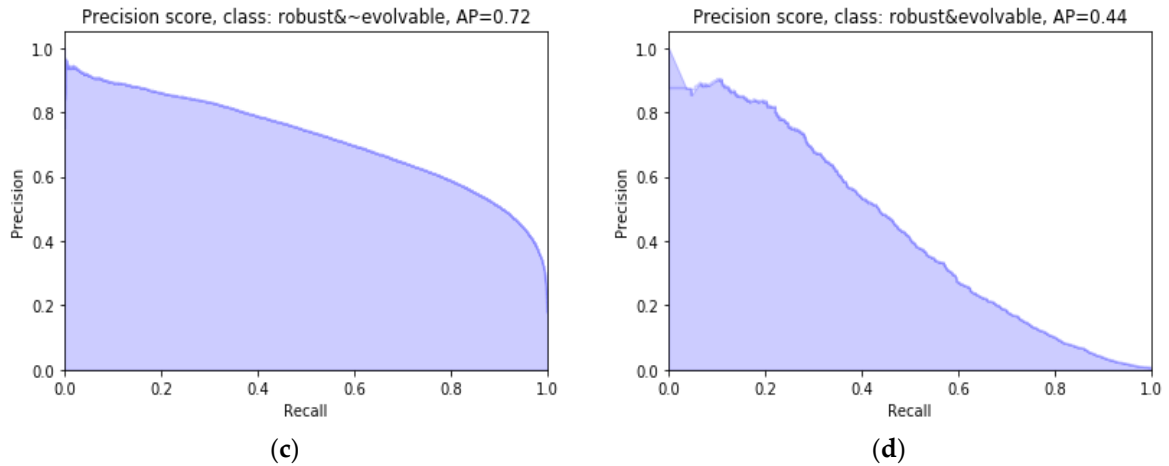


**Figure 9.** Precision-recall curves and average precision scores for the four classes: (a) *not robust & not evolvable*; (b) *not robust & evolvable*; (c) *robust & not evolvable*; (d) *robust & evolvable*.

#### 4. Discussion

In this study, we classified robustness and evolvability in Boolean network models of biological systems into the four classes: *not robust & not evolvable*, *not robust & evolvable*, *robust & not evolvable*, and *robust & evolvable*. The classification was defined based on the change of attractors representing cell fates or functions before and after mutations. We proposed an efficient way to predict the properties of the four classes from the differences of antifragility between original networks and their mutated ones. As a classifier, we used a CNN where the input is the difference of antifragility and the output is the four classes. Our model showed a good performance for the multi-class classification. It indicates that our antifragility measure can play a role of a predictor to estimate the robustness and evolvability of biological networks.

Our classifier with antifragility can be a useful tool for studying the robustness and evolvability of biological networks, especially large Boolean network models. In Boolean networks, finding all attractors is computationally expensive because the state space size exponentially increases as the number of nodes grows. Meanwhile, our antifragility measure focuses on the dynamics during state transitions following external perturbations. Because it is simply calculated from partial information of transient states, it is so efficient to use antifragility as a predictor in the aspect of a computational cost. Also, this finding supports that dynamics during the transient phase following a disturbance can provide meaningful information [73, 74].

For further study, we will use more data, different CNN architectures, and hyperparameter tuning techniques. Because many factors such as the amount of data, complexity of architectures, optimizers, and sampling techniques have an influence on model performance, we will run simulations with various experimental conditions and find the better classifier. Besides, we will thoroughly explore the relationship between antifragility and robustness/evolvability. Here we found that antifragility is closely related to the robustness and evolvability of biological networks. Taking a step forward from this, we will evolve random networks using antifragility as a fitness function and examine robustness and evolvability of evolved networks. This future research could give a clue to the mechanism of how biological systems obtained robustness and evolvability, and also suggest a possibility for developing robust and/or evolvable engineered systems which have antifragility as a control parameter.

#### References

1. De Visser, J. A. G.; Hermisson, J.; Wagner, G. P.; Meyers, L. A.; Bagheri-Chaichian, H.; Blanchard, J. L.; Chao, L.; Cheverud, J. M.; Elena, S. F.; Fontana, W., Perspective: evolution and detection of genetic robustness. *Evolution* **2003**, *57*, (9), 1959-1972.

2. Kirschner, M.; Gerhart, J., Evolvability. *Proceedings of the National Academy of Sciences* **1998**, *95*, (15), 8420-8427.
3. Nehaniv, C. L., Evolvability. *BioSystems* **2003**, *2*, (69), 77-81.
4. Poole, A. M.; Phillips, M. J.; Penny, D., Prokaryote and eukaryote evolvability. *Biosystems* **2003**, *69*, (2-3), 163-185.
5. Stelling, J.; Sauer, U.; Szallasi, Z.; Doyle III, F. J.; Doyle, J., Robustness of cellular functions. *Cell* **2004**, *118*, (6), 675-685.
6. Wagner, A., *Robustness and evolvability in living systems*. 1st ed.; Princeton university press: Princeton, United States, 2007; Vol. 24.
7. Wagner, A., Robustness and evolvability: a paradox resolved. *Proceedings of the Royal Society B: Biological Sciences* **2007**, *275*, (1630), 91-100.
8. Masel, J.; Trotter, M. V., Robustness and evolvability. *Trends in Genetics* **2010**, *26*, (9), 406-414.
9. Partha, R.; Raman, K., Revisiting robustness and evolvability: Evolution in weighted genotype spaces. *PloS one* **2014**, *9*, (11), e112792.
10. Elena, S. F.; Sanjuán, R., The effect of genetic robustness on evolvability in digital organisms. *BMC evolutionary biology* **2008**, *8*, (1), 284.
11. Whitacre, J. M., Degeneracy: a link between evolvability, robustness and complexity in biological systems. *Theoretical Biology and Medical Modelling* **2010**, *7*, (1), 6.
12. Kitano, H., Biological robustness. *Nature Reviews Genetics* **2004**, *5*, (11), 826.
13. Levine, M.; Tjian, R., Transcription regulation and animal diversity. *Nature* **2003**, *424*, (6945), 147.
14. Aldana, M.; Balleza, E.; Kauffman, S.; Resendiz, O., Robustness and evolvability in genetic regulatory networks. *Journal of theoretical biology* **2007**, *245*, (3), 433-448.
15. Chang, H. H.; Hemberg, M.; Barahona, M.; Ingber, D. E.; Huang, S., Transcriptome-wide noise controls lineage choice in mammalian progenitor cells. *Nature* **2008**, *453*, (7194), 544.
16. Huang, S.; Eichler, G.; Bar-Yam, Y.; Ingber, D. E., Cell fates as high-dimensional attractor states of a complex gene regulatory network. *Physical review letters* **2005**, *94*, (12), 128701.
17. Huang, S., Gene expression profiling, genetic networks, and cellular states: an integrating concept for tumorigenesis and drug discovery. *Journal of molecular medicine* **1999**, *77*, (6), 469-480.
18. Kim, H.; Sayama, H. In *Robustness and Evolvability of Multilayer Gene Regulatory Networks*, The 2018 Conference on Artificial Life, Tokyo, Japan, July 23rd-27th, 2018; Ikegami, T.; Virgo, N.; Witkowski, O.; Oka, M.; Suzuki, R.; Iizuka, H., Eds. MIT Press: Tokyo, Japan, 2018; pp 546-547.
19. Kim, J.; Vandamme, D.; Kim, J.-R.; Munoz, A. G.; Kolch, W.; Cho, K.-H., Robustness and evolvability of the human signaling network. *PLoS computational biology* **2014**, *10*, (7), e1003763.
20. Torres-Sosa, C.; Huang, S.; Aldana, M., Criticality is an emergent property of genetic networks that exhibit evolvability. *PLoS computational biology* **2012**, *8*, (9), e1002669.
21. Kim, H.; Sayama, H. In *Robustness and evolvability of multilayer gene regulatory networks*, Artificial Life Conference Proceedings, 2018; MIT Press: 2018; pp 546-547.
22. Taleb, N. N., *Antifragile: Things that gain from disorder*. 1st ed.; Random House Incorporated: New York, United States, 2012; Vol. 3.
23. Pineda, O. K.; Kim, H.; Gershenson, C., A Novel Antifragility Measure Based on Satisfaction and Its Application to Random and Biological Boolean Networks. *Complexity* **2019**, 2019.
24. Kim, H.; Pineda, O. K.; Gershenson, C., A Multilayer Structure Facilitates the Production of Antifragile Systems in Boolean Network Models. *Complexity* **2019**, 2019, 1-11.

25. Kauffman, S. A., Metabolic stability and epigenesis in randomly constructed genetic nets. *Journal of theoretical biology* **1969**, 22, (3), 437-467.
26. Kauffman, S. A., *The origins of order: Self-organization and selection in evolution*. 1st ed.; Oxford University Press: New York, United States, 1993.
27. Kauffman, S., *At home in the universe: The search for the laws of self-organization and complexity*. Reprint ed.; Oxford University Press: New York, United States, 1996.
28. Kim, H.; Sayama, H., The role of criticality of gene regulatory networks in morphogenesis. *IEEE Transactions on Cognitive and Developmental Systems* **2018**.
29. Escobar, L. A.; Kim, H.; Gershenson, C., Effects of Antimodularity and Multiscale Influence in Random Boolean Networks. *Complexity* **2019**, 2019.
30. Poblano-Balp, R.; Gershenson, C., Modular random Boolean networks. *Artificial Life* **2011**, 17, (4), 331-351.
31. Gershenson, C. In *Updating schemes in random Boolean networks: Do they really matter*, Artificial Life IX Proceedings of the Ninth International Conference on the Simulation and Synthesis of Living Systems, 2004; MIT Press: 2004; pp 238-243.
32. Roli, A.; Manfroni, M.; Pincioli, C.; Birattari, M. In *On the design of Boolean network robots*, European Conference on the Applications of Evolutionary Computation, 2011; Springer: 2011; pp 43-52.
33. Muñoz, S.; Carrillo, M.; Azpeitia, E.; Rosenblueth, D. A., Griffin: A Tool for Symbolic Inference of Synchronous Boolean Molecular Networks. *Frontiers in genetics* **2018**, 9, 39.
34. Azpeitia, E.; Muñoz, S.; González-Tokman, D.; Martínez-Sánchez, M. E.; Weinstein, N.; Naldi, A.; Álvarez-Buylla, E. R.; Rosenblueth, D. A.; Mendoza, L., The combination of the functionalities of feedback circuits is determinant for the attractors' number and size in pathway-like Boolean networks. *Scientific reports* **2017**, 7, 42023.
35. Giacomantonio, C. E.; Goodhill, G. J., A Boolean model of the gene regulatory network underlying Mammalian cortical area development. *PLoS computational biology* **2010**, 6, (9), e1000936.
36. Orlando, D. A.; Lin, C. Y.; Bernard, A.; Wang, J. Y.; Socolar, J. E.; Iversen, E. S.; Hartemink, A. J.; Haase, S. B., Global control of cell-cycle transcription by coupled CDK and network oscillators. *Nature* **2008**, 453, (7197), 944.
37. Fauré, A.; Naldi, A.; Chaouiya, C.; Thieffry, D., Dynamical analysis of a generic Boolean model for the control of the mammalian cell cycle. *Bioinformatics* **2006**, 22, (14), e124-e131.
38. Mbodj, A.; Junion, G.; Brun, C.; Furlong, E. E.; Thieffry, D., Logical modelling of Drosophila signalling pathways. *Molecular BioSystems* **2013**, 9, (9), 2248-2258.
39. Steinway, S. N.; Biggs, M. B.; Loughran Jr, T. P.; Papin, J. A.; Albert, R., Inference of network dynamics and metabolic interactions in the gut microbiome. *PLoS computational biology* **2015**, 11, (6), e1004338.
40. Jenkins, A.; Macauley, M., Bistability and Asynchrony in a Boolean Model of the L-arabinose Operon in Escherichia coli. *Bulletin of mathematical biology* **2017**, 79, (8), 1778-1795.
41. Veliz-Cuba, A.; Stigler, B., Boolean models can explain bistability in the lac operon. *Journal of computational biology* **2011**, 18, (6), 783-794.
42. Ortiz-Gutiérrez, E.; García-Cruz, K.; Azpeitia, E.; Castillo, A.; de la Paz Sanchez, M.; Álvarez-Buylla, E. R., A dynamic gene regulatory network model that recovers the cyclic behavior of Arabidopsis thaliana cell cycle. *PLoS computational biology* **2015**, 11, (9), e1004486.

43. Grieb, M.; Burkovski, A.; Sträng, J. E.; Kraus, J. M.; Groß, A.; Palm, G.; Kühl, M.; Kestler, H. A., Predicting variabilities in cardiac gene expression with a boolean network incorporating uncertainty. *PLoS one* **2015**, *10*, (7), e0131832.
44. Herrmann, F.; Groß, A.; Zhou, D.; Kestler, H. A.; Kühl, M., A boolean model of the cardiac gene regulatory network determining first and second heart field identity. *PLoS one* **2012**, *7*, (10), e46798.
45. Rodríguez, A.; Torres, L.; Juárez, U.; Sosa, D.; Azpeitia, E.; García-de Teresa, B.; Cortés, E.; Ortíz, R.; Salazar, A. M.; Ostrosky-Wegman, P., Fanconi anemia cells with unrepaired DNA damage activate components of the checkpoint recovery process. *Theoretical Biology and Medical Modelling* **2015**, *12*, (1), 19.
46. Von der Heyde, S.; Bender, C.; Henjes, F.; Sonntag, J.; Korf, U.; Beissbarth, T., Boolean ErbB network reconstructions and perturbation simulations reveal individual drug response in different breast cancer cell lines. *BMC systems biology* **2014**, *8*, (1), 75.
47. Gupta, S.; Bisht, S. S.; Kukreti, R.; Jain, S.; Brahmachari, S. K., Boolean network analysis of a neurotransmitter signaling pathway. *Journal of theoretical biology* **2007**, *244*, (3), 463-469.
48. Marques-Pita, M.; Rocha, L. M., Canalization and control in automata networks: body segmentation in *Drosophila melanogaster*. *PLoS one* **2013**, *8*, (3), e55946.
49. Irons, D., Logical analysis of the budding yeast cell cycle. *Journal of theoretical biology* **2009**, *257*, (4), 543-559.
50. Martinez-Sanchez, M. E.; Mendoza, L.; Villarreal, C.; Alvarez-Buylla, E. R., A minimal regulatory network of extrinsic and intrinsic factors recovers observed patterns of CD4+ T cell differentiation and plasticity. *PLoS computational biology* **2015**, *11*, (6), e1004324.
51. Saadatpour, A.; Wang, R.-S.; Liao, A.; Liu, X.; Loughran, T. P.; Albert, I.; Albert, R., Dynamical and structural analysis of a T cell survival network identifies novel candidate therapeutic targets for large granular lymphocyte leukemia. *PLoS computational biology* **2011**, *7*, (11), e1002267.
52. Ríos, O.; Frias, S.; Rodríguez, A.; Kofman, S.; Merchant, H.; Torres, L.; Mendoza, L., A Boolean network model of human gonadal sex determination. *Theoretical Biology and Medical Modelling* **2015**, *12*, (1), 26.
53. Sridharan, S.; Layek, R.; Datta, A.; Venkatraj, J., Boolean modeling and fault diagnosis in oxidative stress response. *BMC genomics* **2012**, *13*, (6), S4.
54. Todd, R. G.; Helikar, T., Ergodic sets as cell phenotype of budding yeast cell cycle. *PLoS one* **2012**, *7*, (10), e45780.
55. Sahin, Ö.; Fröhlich, H.; Löbke, C.; Korf, U.; Burmester, S.; Majety, M.; Mattern, J.; Schupp, I.; Chaouiya, C.; Thieffry, D., Modeling ERBB receptor-regulated G1/S transition to find novel targets for de novo trastuzumab resistance. *BMC systems biology* **2009**, *3*, (1), 1.
56. Méndez, A.; Mendoza, L., A network model to describe the terminal differentiation of B cells. *PLoS computational biology* **2016**, *12*, (1), e1004696.
57. Brandon, M.; Howard, B.; Lawrence, C.; Laubenbacher, R., Iron acquisition and oxidative stress response in *Aspergillus fumigatus*. *BMC systems biology* **2015**, *9*, (1), 19.
58. Dahlhaus, M.; Burkovski, A.; Hertwig, F.; Mussel, C.; Volland, R.; Fischer, M.; Debatin, K.-M.; Kestler, H. A.; Beltinger, C., Boolean modeling identifies Greatwall/MASTL as an important regulator in the AURKA network of neuroblastoma. *Cancer letters* **2016**, *371*, (1), 79-89.
59. Mendoza, L.; Xenarios, I., A method for the generation of standardized qualitative dynamical systems of regulatory networks. *Theoretical Biology and Medical Modelling* **2006**, *3*, (1), 13.

60. Silva-Rocha, R.; de Lorenzo, V., The TOL network of *Pseudomonas putida* mt-2 processes multiple environmental inputs into a narrow response space. *Environmental microbiology* **2013**, *15*, (1), 271-286.
61. Thakar, J.; Pathak, A. K.; Murphy, L.; Albert, R.; Cattadori, I. M., Network model of immune responses reveals key effectors to single and co-infection dynamics by a respiratory bacterium and a gastrointestinal helminth. *PLoS computational biology* **2012**, *8*, (1), e1002345.
62. Enciso, J.; Mayani, H.; Mendoza, L.; Pelayo, R., Modeling the pro-inflammatory tumor microenvironment in acute lymphoblastic leukemia predicts a breakdown of hematopoietic-mesenchymal communication networks. *Frontiers in physiology* **2016**, *7*, 349.
63. Ding, S.; Wang, W., Recipes and mechanisms of cellular reprogramming: a case study on budding yeast *Saccharomyces cerevisiae*. *BMC systems biology* **2011**, *5*, (1), 50.
64. Li, F.; Long, T.; Lu, Y.; Ouyang, Q.; Tang, C., The yeast cell-cycle network is robustly designed. *Proceedings of the National Academy of Sciences* **2004**, *101*, (14), 4781-4786.
65. Huitzil, S.; Sandoval-Motta, S.; Frank, A.; Aldana, M., Modeling the Role of the Microbiome in Evolution. *Frontiers in physiology* **2018**, *9*, 1836.
66. Kim, H. The Role of Criticality of Gene Regulatory Networks on Emergent Properties of Biological Systems. Doctoral Dissertation, Binghamton University, May 10, 2018.
67. Santamaría-Bonfil, G.; Gershenson, C.; Fernández, N., A Package for Measuring emergence, Self-organization, and Complexity Based on Shannon entropy. *Frontiers in Robotics and AI* **2017**, *4*, 10.
68. Fernández, N.; Maldonado, C.; Gershenson, C., Information measures of complexity, emergence, self-organization, homeostasis, and autopoiesis. In *Guided self-organization: Inception*, 1st ed.; Prokopenko, M., Ed. Springer: Berlin, Heidelberg, Germany, 2014; pp 19-51.
69. Gershenson, C.; Fernández, N., Complexity and information: Measuring emergence, self-organization, and homeostasis at multiple scales. *Complexity* **2012**, *18*, (2), 29-44.
70. Gershenson, C., The sigma profile: A formal tool to study organization and its evolution at multiple scales. *Complexity* **2011**, *16*, (5), 37-44.
71. Chawla, N. V.; Bowyer, K. W.; Hall, L. O.; Kegelmeyer, W. P., SMOTE: synthetic minority over-sampling technique. *Journal of artificial intelligence research* **2002**, *16*, 321-357.
72. Krawitz, P.; Shmulevich, I., Basin entropy in Boolean network ensembles. *Physical review letters* **2007**, *98*, (15), 158701.
73. Tang, S.; Allesina, S., Reactivity and stability of large ecosystems. *Frontiers in Ecology and Evolution* **2014**, *2*, 21.
74. Arnoldi, J.-F.; Loreau, M.; Haegeman, B., Resilience, reactivity and variability: A mathematical comparison of ecological stability measures. *Journal of theoretical biology* **2016**, *389*, 47-59.